J|A|C|S
ARTICLES
Published on Web 12/13/2002

An Efficient RNA-Cleaving DNA Enzyme that Synchronizes Catalysis with Fluorescence Signaling

Shirley H. J. Mei, Zhongjie Liu, John D. Brennan, and Yingfu Li*

Department of Biochemistry and Department of Chemistry, McMaster University, 1200 Main Street West, Hamilton, Ontario, L8N 3Z5 Canada

Received August 13, 2002; E-mail: liying@mcmaster.ca

Abstract: DNA enzymes are single-stranded DNA molecules with catalytic capabilities that are isolated from random-sequence DNA libraries by "in vitro selection". This new class of catalytic biomolecules has the potential of being used as unique molecular tools in a variety of innovative applications. Here we describe the creation and characterization of an RNA-cleaving autocatalytic DNA, DEC22-18, that uniquely links chemical catalysis with real-time fluorescence signaling capability in the same molecule. A *trans*-acting DNA molecule, DET22-18, was also developed from DEC22-18 that behaves as a true enzyme with a k_{cat} of $\sim$7 min^{-1}—a rate constant that is the second largest ever reported for a DNA enzyme. It cleaves a chimeric RNA/DNA substrate at the lone RNA linkage surrounded by a closely spaced fluorophore-quencher pair—a unique structure that permits the synchronization of the chemical cleavage with fluorescence signaling. DET22-18 has a stem−loop structure and can be conjugated with DNA aptamers to form allosteric deoxyribozyme biosensors.

Introduction

Over the past decade, there have been significant advances in the development of selective biosensors based on the use of DNA as a biorecognition element. While the majority of DNA-based sensors are designed to detect complementary DNA, many recent reports have demonstrated that single-stranded DNA can also form intricate tertiary structures that allow it to selectively bind to non-DNA targets (so-called aptamers)[1,2] or catalyze chemical reactions.[3,4] To date, over 100 DNA sequences have been reported for facilitating many types of chemical transformations.[5] Despite having very limited chemical functionalities, deoxyribozymes that perform catalysis with surprising efficiency have been reported in a number of studies.[6] For example, a small DNA enzyme known as 10-23 performs site-specific RNA cleavage with a very impressive k_{cat} of $\sim$10 min^{-1}.[7] It is clear that the lack of a 2′-hydroxyl group in DNA relative to RNA is not a detriment to catalytic performance. The catalytic capabilities of DNA can be enhanced through the use of metal ions[8] and small-molecule cofactors[9] as well as through the modification with chemical functionalities that are useful for catalysis.[10] Furthermore, when compared to ribozymes, deoxyribozymes are easier to prepare and more resistant to chemical and enzymatic degradation, and therefore, properly engineered and catalytically efficient DNA enzymes are very desirable elements for the construction of rugged biosensors.

A flurry of recent activities and resultant successes in engineering molecular probes made of allosteric ribozymes[11,12] and deoxyribozymes[13] have opened up tremendous opportunities for using catalytic nucleic acids for wide-ranging applications in the diagnostic, biosensing, and drug-screening fields. The

* Author for correspondence. Telephone: (905) 525-9140, ext 22462. Fax: (905) 522-9033.

(1) (a) Ellington, A. D.; Szostak, J. W. *Nature* **1990**, *346*, 818−822. (b) Tuerk, C.; Gold, L. *Science* **1990**, *249*, 505−510.
(2) (a) Famulok, M.; Mayer, G.; Blind, M. *Acc. Chem. Res.* **2001**, *33*, 591−599. (b) Wilson, D. S.; Szostak, J. W. *Annu. Rev. Biochem.* **1999**; *68*, 611−647.
(3) (a) Breaker, R. R. *Nat. Biotechnol.* **1997**, *15*, 427−431. (b) Breaker, R. R. *Science* **2000**, *290*, 2095−2096.
(4) (a) Sen D.; Geyer, C. R. *Curr. Opin. Chem. Biol.* **1998**, *2*, 680−687. (b) Li, Y.; Breaker, R. R. *Curr. Opin. Struct. Biol.* **1999**, *9*, 315−323. (c) Jaschke, A. *Curr. Opin. Struct. Biol.* **2001**, *11*, 321−326, (d) Emilsson, G. M.; Breaker, R. R. *Cell Mol. Life Sci.* **2002**, *59*, 596−607.
(5) (a) Breaker, R. R.; Joyce, G. F. *Chem. Biol.* **1994**, *1*, 223−229. (b) Cuenoud, B.; Szostak, J. W. *Nature* **1995**, *375*, 611−614. (c). Li, Y.; Sen, D. *Nat. Struct. Biol.* **1996**, *3*, 743−747. (d) Carmi, N.; Schultz, L. A.; Breaker, R. R. *Chem. Biol.* **1996**, *3*, 1039−1046. (e) Burmeister, J.; von Kiedrowski, G.; Ellington, A. D. *Angew. Chem., Int. Ed. Engl.* **1997**, *36*, 1321−1324. (f) Travascio, P.; Li, Y.; Sen, D. *Chem. Biol.* **1998**, *5*, 505−517. (g). Li, Y.; Breaker, R. R. *Proc. Natl. Acad. Sci. U.S.A.* **1999**, *96*, 2746−2751. (h). Li, Y.; Liu, Y.; Breaker, R. R. *Biochemistry* **2000**, *39*, 3106−3114. (i). Sheppard, T. L.; Ordoukhanian, P.; Joyce, G. F. *Proc. Natl. Acad. Sci. U.S.A.* **2000**, *97*, 7802−7807. (j) Levy, M.; Ellington, A. D. *Bioorg. Med. Chem.* **2001**, *9*, 2581−2587.
(6) (a) Santoro, S. W.; Joyce, G. F. *Proc. Natl. Acad. Sci. U.S.A.* **1997**, *94*, 4262−6. (b) Li, J.; Zheng, W.; Kwon, A. H.; Lu, Y. *Nucleic Acids Res.* **2000**, *28*, 481−448, (c) Feldman, A. R.; Sen, D. *J. Mol. Biol.* **2001**, *313*, 283−294. (d) Wang, W.; Billen, L. P.; Li, Y. *Chem. Biol.* **2002**, *9*, 507−517.
(7) (a) Reference 5a. (b) Santoro, S. W.; Joyce, G. F. *Biochemistry* **1998**, *37*, 13330−13342.
(8) Reference 6d.
(9) Roth, A.; Breaker, R. R. *Proc. Natl. Acad. Sci. U.S.A.* **1998**, *95*, 6027−6031.
(10) (a) Santoro, S. W.; Joyce, G. F.; Sakthivel, K.; Gramatikova, S.; Barbas, C. F. *J. Am. Chem. Soc.* **2000**, *122*, 2433−2439. (b) Perrin, D. M.; Garestier, T.; Helene, C. *J. Am. Chem. Soc.* **2001**, *123*, 1556−1563. (c) Lermer, L.; Roupioz, Y.; Ting, R.; Perrin, D. M. *J. Am. Chem. Soc.* **2002**, *124*, 9960−9961.
(11) Breaker, R. R. *Curr. Opin. Biotechnol.* **2002**, *13*, 31−39.
(12) (a) Soukup, G. A.; Breaker, R. R. *Proc. Natl. Acad. Sci. U.S.A.* **1999**, *96*, 3584−3589. (b) Robertson, M. P.; Ellington, A. D. *Nat. Biotechnol.* **1999**, *17*, 62−66.
(13) (a) Wang, D. Y.; Sen, D. *J. Mol. Biol.* **2001**, *310*, 723−734. (b) Stojanovic, M. N.; de Prada, P.; Landry, D. W. *Chembiochem* **2001**, *2*, 411−415. (c) Levy, M.; Ellington, A. D. *Chem. Biol.* **2002**, *9*, 417−426. (d) Stojanovic, M. N.; de Prada, P.; Landry, D. W. *Nucleic Acids Res.* **2000**, *28*, 2915−2918.

10.1021/ja0281232 CCC: $25.00

use of deoxyribozymes with fast catalytic rates and large turnover numbers allows for the engineering of effective allosteric DNA enzymes for practical applications where rapid enzymatic action is essential. To engineer catalytic DNA probes for detection-directed applications, it is very desirable to use DNA enzymes that can couple enzymatic activity with fluorescence signaling capability so that easy and fast detection can be performed in real time without the need for time-consuming separation steps.

In the past few years pioneering efforts have led to the engineering of molecular beacon-based[14] DNA enzyme reporters that perform fluorescence signaling by fluorescence-quenching/dequenching[15] or fluorescence-resonance-energy-transfer mechanisms.[16] However, these reporters have been engineered using existing DNA enzymes that were not created specifically for signaling applications, and as a result the sensor molecules created are not optimized in catalytic rate or signaling properties to achieve high sensitivity. Therefore, our goal was to create a de novo fluorescence-generating RNA-cleaving DNA enzyme system that (1) maintains low background fluorescence under any condition, (2) is capable of generating a very large fluorescent signal upon RNA cleavage by coupling this process to a dequenching mechanism, and (3) exhibits a very large catalytic rate constant. Herein, we describe the creation and characterization of an efficient RNA-cleaving DNA enzyme that uniquely links chemical catalysis with real-time fluorescence signaling capability. Two examples of this system, a *cis*-acting enzyme capable of autocatalysis, and a *trans*-acting enzyme that acts on a specific chimeric substrate, are described. Development of an allosteric DNA enzyme controlled by ATP binding is also demonstrated on the basis of the conjugation of a known ATP aptamer[17] to the *cis*-acting enzyme.

Experimental Section

Materials. Standard oligonucleotides were prepared by automated DNA synthesis using cyanoethylphosphoramidite chemistry (Keck Biotechnology Resource Laboratory, Yale University; Central Facility, McMaster University). Random-sequence DNA libraries were synthesized using an equimolar mixture of the four standard phosphoramidites. DNA oligonucleotides were purified by 10% preparative denaturing (8 M urea) polyacrylamide gel electrophoresis (PAGE), and their concentrations were determined spectroscopically and calculated using the Biopolymer Calculator program.[18]

Fluorescein and 4-(4-dimethylaminophenylazo)benzoic acid (DABCYL) labels were incorporated into the DNA library during automated DNA synthesis using Fluorescein-dT amidite and DABCYL-dT amidite (Glen Research, Sterling, Virginia). The adenine ribonucleotide linkage was also introduced during solid-state synthesis using A-TOM-CE Phosphoramidite (Glen Research). Fluorescein- and DABCYL-modified oligonucleotides were purified by reverse phase liquid chromatography (HPLC) performed on a Beckman Coulter HPLC System Gold with a 168 diode array detector. The HPLC column used was an Agilent Zorbax ODS C18 column with dimensions of 4.6 mm × 250 mm and a 5-μm bead diameter. Elution was achieved using a two-buffer system with buffer A being 0.1 M triethylammonium acetate (TEAA, pH 6.5) and buffer B being pure acetonitrile. The best separation results were achieved using a nonlinear elution gradient (0% B for 5 min, 10% B to 30% B over 95 min) at a flow rate of 0.5 mL/min. The main peak was found to have very strong absorption at both 260 and 491 nm.

The TOM protective group on the 2′-hydroxyl group of the RNA linkage was removed by incubation with 150 μL of 1 M tetrabutylammonium fluoride (TBAF) in THF at 60 °C with shaking for 6 h, followed by the addition of 250 μL of 100 mM Tris (pH 8.3) and further incubation with shaking for 30 min at 37 °C. The DNA was recovered using ethanol precipitation and dissolved in water containing 0.01% SDS; the tetrabutylammonium salt was removed by centrifugation using a spin column (Nanosep 3K Omega, Pall Corp., Ann Arbor, Michigan).

Nucleoside 5′-triphosphates, [γ-^{32}P]ATP and [α-^{32}P]dGTP were purchased from Amersham Pharmacia. *Taq* DNA polymerase, T4 DNA ligase, and T4 polynucleotide kinase (PNK) were purchased from MBI Fermentas. All other chemical reagents were purchased from Sigma.

In Vitro Selection Procedures. 5′-Phosphorylated, gel-purified, 86-nt random-sequence DNA L1 (300 pmol) was mixed in an equimolar ratio with template T1 and acceptor A1 (all sequences shown in Figure 2B), heated to 90 °C for 30 s, cooled to room temperature, and combined with ligase buffer and T4 DNA ligase for DNA ligation to introduce the modified DNA domain. The ligation mixture (50 μL) contained 50 mM Tris-HCl (pH 7.8 at 23 °C), 40 mM NaCl, 10 mM $MgCl_2$, 1 mg/mL BSA, 0.5 mM ATP, and 0.1 units (Weiss) μL^{-1} T4 DNA ligase. The solution was incubated at 23 °C for 1 h, and the ligated 109-nt DNA was purified by 10% denaturing PAGE.

The 109-nt DNA population constructed as above was used as the initial pool (denoted generation 0 or G0), which was heated to 90 °C for 30 s, cooled to room temperature, and then combined with a 2× selection buffer (100 mM HEPES, pH 6.8 at 23 °C, 800 mM NaCl, 200 mM KCl, 15 mM $MgCl_2$, 10 mM $MnCl_2$, 2.5 mM $CdCl_2$, 2 mM $CoCl_2$, 0.5 mM $NiCl_2$) to a final DNA concentration of 0.05 μM. The mixture was incubated for self-cleavage at 23 °C for 5 h.

The cleavage reaction was stopped by the addition of EDTA (pH 8.0) to a final concentration of 30 mM. The cleaved DNA was isolated by 10% denaturing PAGE. To increase the yield of DNA recovery and to track the status of 94-nt cleaved product, 0.25 pmol of highly radioactive 94-nt DNA marker, made by alkaline digestion of the 109-nt construct, was used as the "carrier DNA". The isolated cleavage product was amplified by PCR in 5 × 100 μL reaction volume using primers P1 and P2 (Figure 2B). The PCR reaction was monitored in real-time using SYBR Green (Molecular Probes). The amplified DNA product (2%) was used as the DNA template for a second PCR reaction in a 10 × 100 μL reaction volume using primer P1 and ribo-terminated primer P3 (Figure 2B). The reaction mixture also included 30 μCi of [α-^{32}P]dGTP for DNA labeling.

The DNA product in the second PCR was recovered by ethanol precipitation, resuspended in 90 μL of 0.25 M NaOH and incubated at 90 °C for 10 min to cleave the single embedded RNA linkage. The cleavage solution was neutralized by adding 10 μL of 3 M NaOAc (pH 5.2 at 23 °C), and the 86-nt single-stranded DNA fragments were isolated by denaturing 10% PAGE. The recovered DNA molecules were incubated with 10 units of PNK at 37 °C for 1 h for DNA phosphorylation in a 100-μL reaction mixture containing 50 mM Tris-HCl (pH 7.8 at 23 °C), 40 mM NaCl, 10 mM $MgCl_2$, 1 mg/mL BSA, and 0.84 μM [γ-^{32}P]ATP (70 μCi). The 5′-phosphorylated DNA was used for the second round of selection using the same procedure described for the first round of selection.

A total of 22 rounds of selection and amplification were carried out. The third and subsequent rounds of selection were conducted in the same way as described for the first round except that (1) the scale of the self-cleavage reaction, PCR, DNA phosphorylation, and DNA ligation reactions was all reduced by 5-fold, (2) the self-cleavage time was shortened from 5 h (G0−G11), to 10 min (G12), to 1 min (G13), to 30 s (G14 and G15), to 5 s (G16 and G17), and finally to 1 s (G18−G22), and (3) the "carrier DNA" was not used.

(14) Tyagi, S.; Kramer, F. R. *Nat. Biotechnol*. **1996**, *14*, 303−308.
(15) Li, J.; Lu, Y. *J. Am. Chem. Soc.* **2000**, *122*, 1046−1047.
(16) (a) Todd, A. V.; Fuery, C. J.; Impey, H. L.; Applegate, T. L.; Haughton, M. A. *Clin. Chem*. **2000**, *46*, 625−630. (b) Stojanovic, M. N.; Mitchell, T. E.; Stefanovic, D. *J. Am. Chem. Soc.* **2002** *124*, 3555−3561. (c) Reference 13b.
(17) Huizenga, D. E.; Szostak, J. W. *Biochemistry* **1995**, *34*, 656−665.
(18) It can be accessed at http://paris.chem.yale.edu/extinct.frames.html.

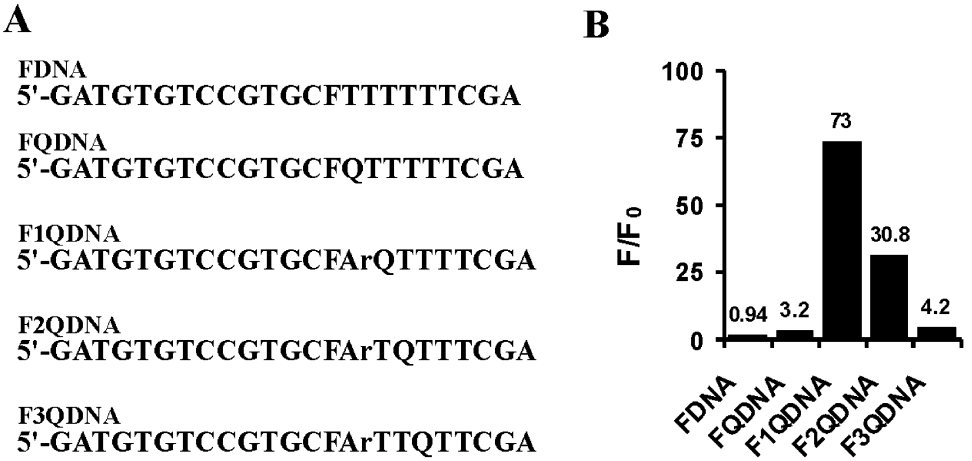

Figure 1. Examination of the signaling capability of DNA oligonucleotides modified with a fluorophore, a quencher, or a ribonucleotide. (A) DNA sequences used. F: fluorescein-dT; Q: DABCYL-dT; Ar: adenine ribonucleotide. (B) Fluorescence enhancement of each DNA molecule following a 20-h incubation in the presence of 0.25 M NaOH. 0.5 M NaOH was combined with an equal volume of a DNA solution containing either 80 nM of FDNA, FQDNA, F1QDNA, F2QDNA, or F3QDNA. The fluorescence intensity of each mixture was recorded twice: one measurement was taken immediately following the addition of NaOH (F_0) and the other after a 20-h incubation at room temperature (F).

Cloning and Sequencing of Selected Deoxyribozymes. DNA sequences from the 22nd round of selection were amplified by PCR and cloned into a vector by the TA cloning method. The plasmids containing individual catalysts were prepared using a Qiagen MiniPrep Kit. DNA sequencing was performed on an LCQ2000 capillary DNA sequencer (Beckman Coulter), following the procedures recommended by the manufacturer.

Fluorescence Measurements. All measurements were taken from 400-μL solutions on a Cary Eclipse fluorescence spectrophotometer (Varian). The excitation was set at 490 nm, and emission, at 520 nm.

Kinetic Analyses. A typical reaction involved the following steps: (1) heat denaturation of DNA in water for 30 s at 90 °C, (2) incubation for RNA cleavage at room temperature in a reaction buffer for a designated time, (3) addition of EDTA to 30 mM to stop the reaction, (4) separation of cleavage products by denaturing 10% PAGE, and (5) quantitation using a PhosphoImager and ImageQuant software (Molecular Dynamics). Aliquots of an RNA cleavage reaction solution were collected at different reaction time points, and the rate constant for the reaction was determined by plotting the natural logarithm of the fraction of DNA that remained unreacted versus the reaction time. The negative slope of the line, obtained from points within the first 10% of the reaction and produced by a least-squares fit, was taken as the rate constant.

Results

Design of Oligonucleotides for Optimal Fluorescence Quenching. We sought to create an RNA-cleavage-based signaling DNA enzyme reporter that had a low background fluorescence in its inactive state under any conditions but that could generate a large fluorescence signal upon cleavage of the single RNA linkage embedded in a DNA chain and flanked by a covalently linked fluorophore and quencher pair. This arrangement not only results in very efficient fluorescence quenching because of the short distance between the fluorophore and the quencher, but also minimizes false positives because the quencher cannot be separated from the fluorophore until the RNA linkage is cleaved. To determine the optimal distance between the fluorophore and the quencher, we synthesized a series of DNA oligonucleotides with the modifications as shown in Figure 1A (F: fluorescein-dT; Q: DABCYL-dT; Ar: adenine ribonucleotide). The cleavage-dependent signaling behavior of these DNA molecules was assessed by treatment with 0.25 M NaOH (Figure 1B), where F_0 and F are the fluorescence intensities of a relevant DNA solution measured immediately after the addition of 0.25 M NaOH (RNA cleavage yet to occur) and after incubation for 20 h (full RNA cleavage[19]). F1QDNA had the most significant fluorescence change (with an increase in intensity of ~70-fold), followed by F2QDNA (~30-fold). In contrast, F3QDNA produced a much smaller fluorescence enhancement of only 4-fold. The decrease in fluorescence-enhancement when the fluorophore and quencher were moved further apart on the molecule resulted in a higher background (F_0) as the distance between them increased, owing to less efficient quenching. All FxQDNA systems ($x = 1-3$) reached final intensity values that were similar to that of FDNA. The small increase in intensity for FQDNA (no RNA linker) likely resulted from a slow base-catalyzed hydrolysis reaction that removed either the F or Q moiety from the DNA backbone.

Since F1QDNA had the largest fluorescence intensity increase, a cleavage system built with such a modification should be the most sensitive in terms of signal generation. For this reason, a ribonucleotide immediately flanked by a fluorophore-modified nucleotide and a quencher-modified nucleotide was incorporated into the starting random-sequence pool to be used for the creation of DNA enzymes.

In Vitro Selection. We employed the selection scheme shown in Figure 2A to isolate signaling autocatalytic DNA molecules. In step I, a pool of single-stranded 86-nt DNA containing 43 random-sequence nucleotides was first ligated to the acceptor DNA A1 (23-nt) containing the three key moieties described above (all DNA sequences are given in Figure 2B). The ligated 109-nt DNA was purified by PAGE in step II, followed by step III where the modified DNA molecules were incubated with several divalent metal ion cofactors (see Discussion below). Any autocatalytic DNA capable of cleaving the lone RNA linkage was expected to generate a 94-nt DNA fragment that could be isolated by PAGE in step IV. The recovered DNA was amplified by two successive polymerase chain reactions (PCR). The first PCR was carried out with the use of primers P1 and P2 (step V). The second PCR (step VI) used P1 and P3. Since P3 was

(19) Li, Y.; Breaker, R. R. *J. Am. Chem. Soc.* **1999**, *121*, 5364−5372.

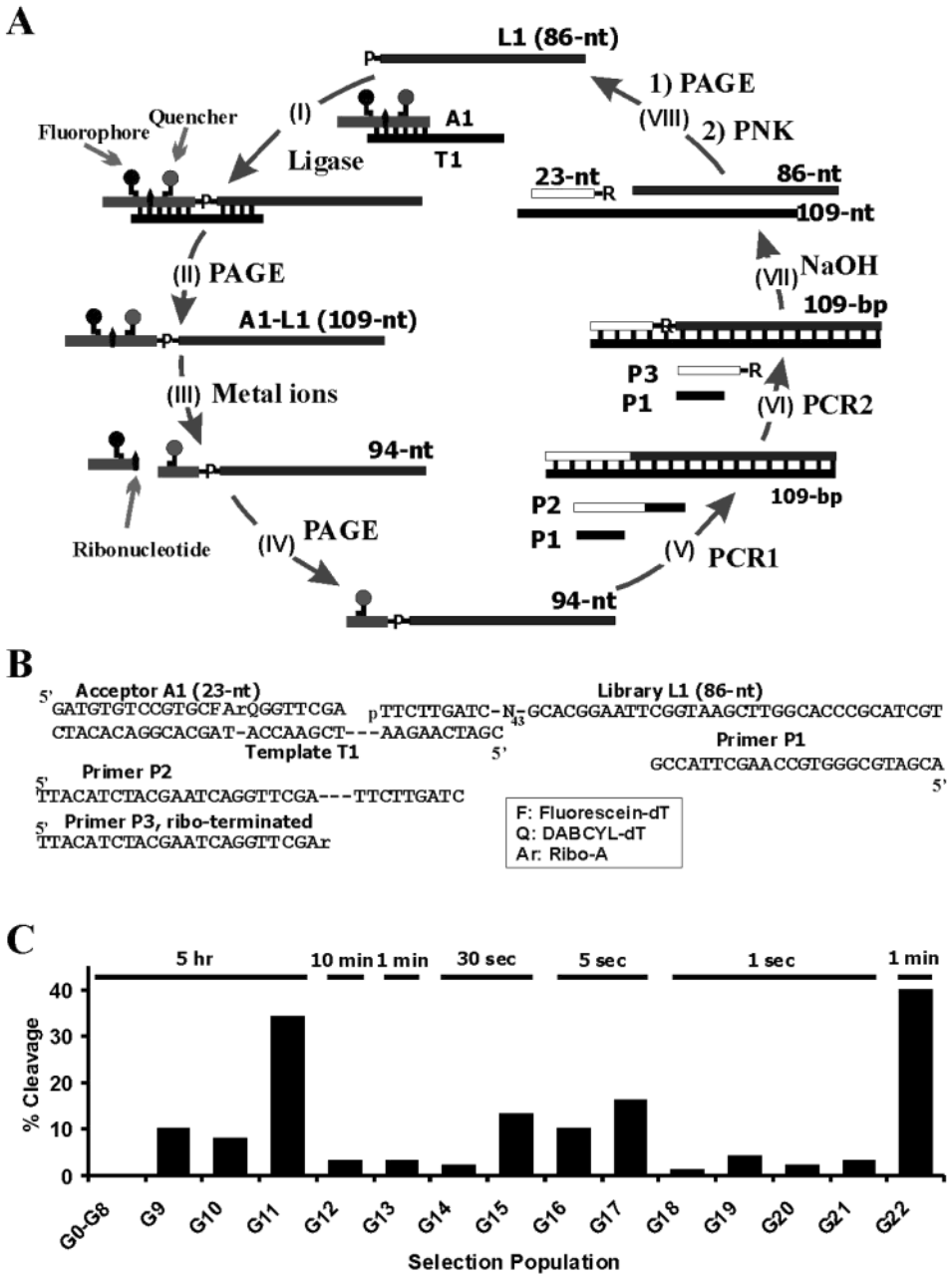

Figure 2. Selection of autocatalytic DNAs. (A) Selection scheme. Each selection cycle consists of steps I−VIII. (I) 86-nt DNA is ligated to acceptor DNA A1. (II) Ligated 109-nt DNA is isolated by PAGE. (III) Purified DNA is incubated with divalent metal ions for RNA cleavage. (IV) 94-nt cleavage fragment is isolated by PAGE. (V) The recovered 94-nt DNA is amplified by PCR using primers P1 and P2. (VI) 109-bp PCR product in (V) is re-amplified using primers P1 and P3 to introduce a ribonucleotide linkage embedded within DNA. (VII) The resulting double-stranded DNAs are treated with NaOH to cleave the RNA linkage. (VIII) 86-nt cleavage fragment is purified by PAGE, phosphorylated at the 5′-end, and used to initiate the next round. (B) Sequences of the DNA pool (L1), acceptor A1, and template T1, and the primers for PCR. N43 is the random domain. (C) Selection progress. The percentage of molecules that underwent cleavage of the RNA linkage in each selection round is plotted. The reaction time for each round is indicated on the top of the graph. Detailed experimental procedures are described in the Experimental Section. The 1-min cleavage product from G22 DNA was used for DNA cloning.

a ribo-terminated primer, the double-stranded DNA product generated in the second PCR step contained a single ribonucleotide linkage in the deoxyribozyme-containing strand. The DNA product from the second PCR was treated with NaOH (step VII) under conditions that could fully cleave the ribonucleotide linkage (0.25 M NaOH, 90 °C, 10 min). The digested DNA mixture was subjected to PAGE purification and DNA phosphorylation (step VIII), with the 5′-phosphorylated DNA used to initiate the next round of selection.

To facilitate the creation of DNA enzymes, we used Mg^{2+} and several divalent transition metal ions including Mn^{2+}, Co^{2+}, Ni^{2+}, and Cd^{2+} in the selection buffer. The use of divalent transition metal ions was based on a recent study demonstrating that the use of these metal ions could lead to the isolation of diverse deoxyribozymes from a random-sequence pool.[8] However, the choice of the specific divalent transition metal ions in our study was rather arbitrary. The total concentration of divalent metal ions was chosen to be 15 mM with individual concentrations set at the following: 7.5 mM Mg^{2+}, 5 mM Mn^{2+}, 1.25 mM Cd^{2+}, 1 mM Co^{2+}, 0.25 mM Ni^{2+}. It was decided to use lower concentrations of Cd^{2+}, Co^{2+}, or Ni^{2+} on the basis of their demonstrated inhibitory effect on a Ca^{2+}-dependent self-

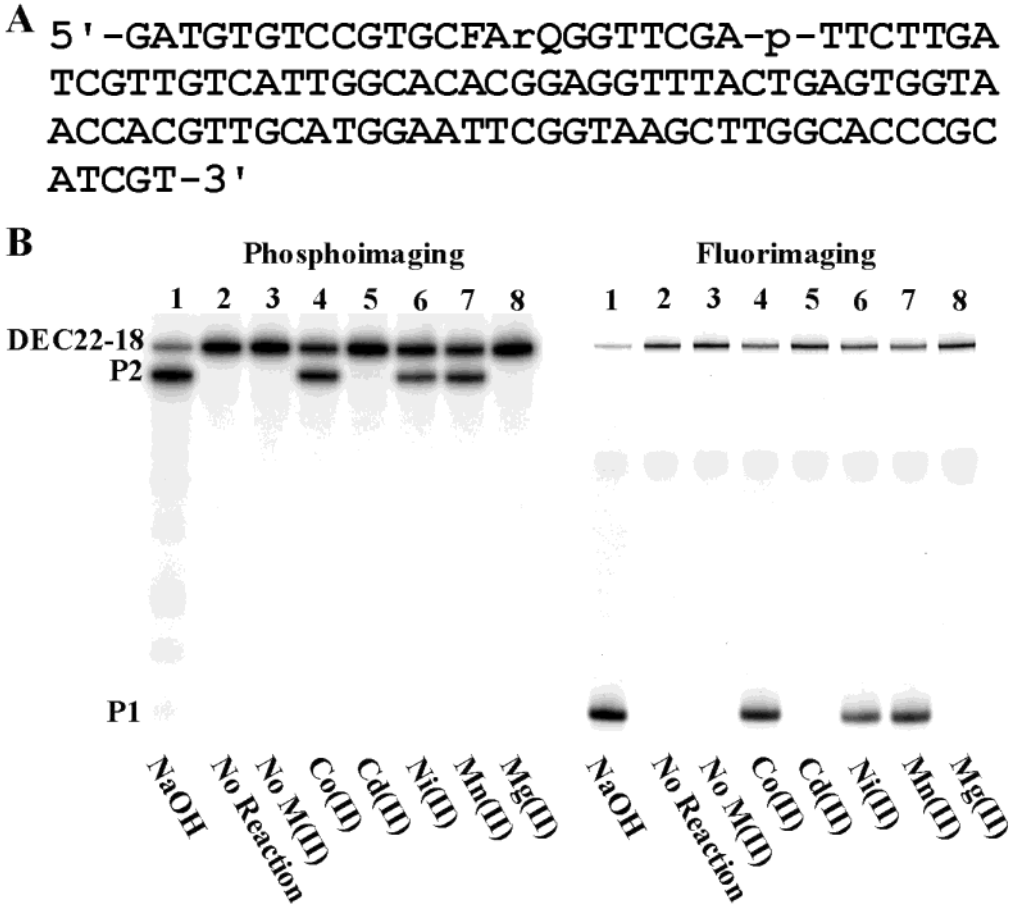

Figure 3. DEC22-18 and its metal specificity. (A) The sequence of DEC22-18. (B) Confirmation of catalytic activity and determination of metal ion specificity. The 86-nt synthetic DNA molecule DEC22-18A (corresponding to the sequence domain after the letter "p" in 3A) was first phosphorylated at the 5′-end with [γ-^{32}P]ATP and then ligated to 23-nt substrate A1. After gel purification, the 109-nt, full-length DNA molecule was heated at 90 °C for 30 s, cooled to room temperature, and then tested for RNA cleavage (lanes 3−8) under various solution conditions. The reaction buffers contained 0.3 μM DEC22-18, 50 mM HEPES (pH6.8), 400 mM NaCl, and 100 mM KCl, and divalent metal ions specified as follows: no divalent metal ions (lane 3), 1 mM $CoCl_2$ and 14 mM $MgCl_2$ (lane 4), 1.25 mM $CdCl_2$ and 13.75 mM $MgCl_2$ (lane 5), 0.25 mM $NiCl_2$ and 14.75 mM $MgCl_2$ (lane 6), 5 mM $MnCl_2$ and 10 mM $MgCl_2$ (lane 7), and 15 mM $MgCl_2$ (lane 8). The cleavage reaction was stopped after 10 min with the addition of EDTA to reach 30 mM. The cleaved products were separated from the uncleaved precursor by denaturing 10% PAGE. The phosphorimage was obtained using a Storm 820 Phosphoimager (Molecular Dynamics). The fluoroimage was obtained using a Typhoon 9200 (Molecular Dynamics). The excitation wavelength was 532 nm (green laser), and emission was monitored at >535 nm using a long-pass filter. P1 and P2 correspond to the 5′ and 3′ cleavage products, respectively.

phosphorylating DNA (Achenbach and Li, unpublished data). To minimize the potential inhibitory effect of these metal ions in this selection, they were used at their respective IC_{50} concentrations determined in the above-mentioned study. The concentrations of Mg^{2+} and Mn^{2+} were used at higher concentrations since these two metal ions were not found to inhibit the activity of the self-phosphorylating deoxyribozymes at concentrations as high as 25 mM.

The selection progress is summarized in Figure 2C. No detectable cleavage activity was observed for DNA sequences isolated in generations G0−G8. However, significant cleavage was seen in G9 and G10. By G11, more than 30% of the DNA construct was cleaved after a 5-h incubation (Figure 2C). The reaction time was then progressively reduced to isolate very efficient DNA enzymes. The self-cleavage reaction was first allowed only to proceed for 10 min in G12 and 1 min in G13, and the reaction time was further reduced to 30 s in G14 and G15, to 5 s in G16 and G17, and finally to about 1 s in G18−G22. The DNA molecules in G22 were also allowed to react for 1 min, and the cleaved DNA was cloned using the method described previously.[8]

Verification of Catalytic Activity. A single class of deoxyribozyme was found in the G22 pool after we sequenced more than 20 clones. The sequence of this autocatalytic DNA molecule, named DEC22-18,[20] is given in Figure 3A. The confirmation of its catalytic activity and the analysis of its metal ion requirements are shown in Figure 3B. We labeled the DNA enzyme at the phosphodiester bond linking the 23rd and 24th nucleotides with ^{32}P. Therefore, the uncleaved 109-nt DEC22-18 is weakly fluorescent (since the Q moiety is still present) and highly radioactive. Upon self-cleavage, DEC22-18 should give rise to two cleavage products, with the 5′ cleaved fragment (15-nt; P1) being strongly fluorescent but not radioactive and the 3′ fragment (94-nt; P2) being only radioactive. The two cleavage products were obtained by the partial digestion of the deoxyribozyme with NaOH and used as the control (lane 1). When the deoxyribozyme was treated with water (lane 2), monovalent metal ions (lane 3), Cd^{2+} (lane 5), or Mg^{2+} (lane

(20) This DNA sequence was identified as the 18th clone in the generation 22. To follow the tradition originated in ref 5a, we named our DNA enzyme as DEC22-18 where DE stands for DNA enzyme, C for *cis*-acting (similarly, T for *trans*-acting).

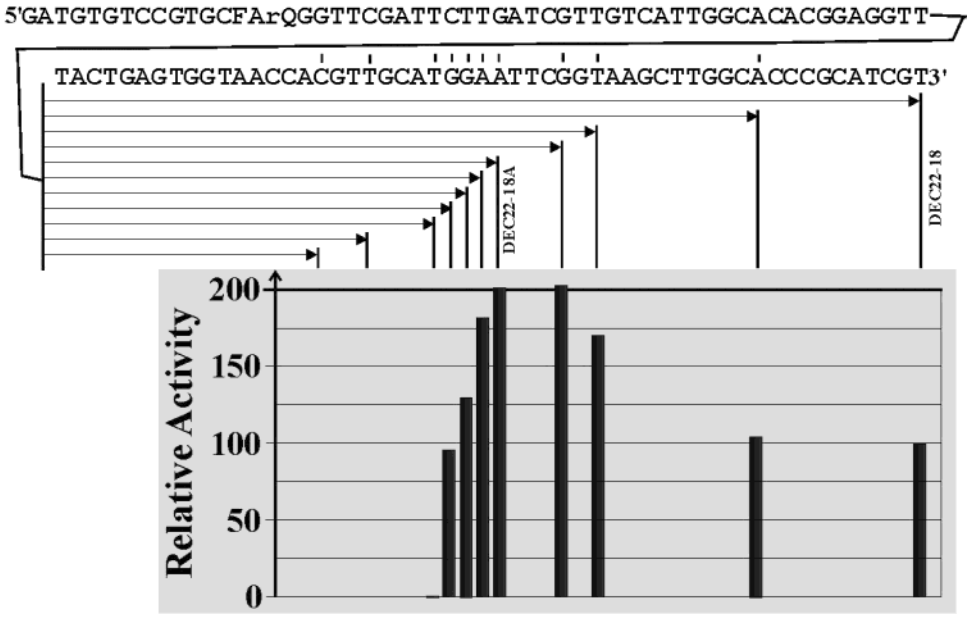

Figure 4. Sequence truncation of DEC22-18. All 3′ truncated mutants of DEC22-18 were assessed for relative cleavage capabilities under the following reaction conditions: 50 mM HEPES (pH 6.8 at 23 °C), 400 mM NaCl, 100 mM KCl, 7.5 mM $MgCl_2$, 5 mM $MnCl_2$, 1.25 mM $CdCl_2$, 1 mM $CoCl_2$, 0.25 mM $NiCl_2$. Approximately 5 nM of each candidate deoxyribozyme was treated for self-cleavage at room temperature. The rate constants of the mutants were normalized against the wild-type DEC22-18 (which was taken as 100) and plotted in the embedded graph.

8), no cleavage product was produced; when the DNA enzyme was treated with Co^{2+} (lane 4), Ni^{2+} (lane 6), or Mn^{2+} (lane 7), it self-cleaved into the two expected DNA fragments with the matching signaling properties. In each case, the ratio of fluorescence intensity of P1 over that of uncleaved DEC22-18 was significantly larger than the ratio of radioactivity for these species, signifying a fluorescence enhancement consistent with the coupled catalysis-signaling mechanism. The data indicate that DEC22-18 is a metallo-DNA enzyme capable of using Co(II), Ni(II), or Mn(II) as its divalent metal cofactor. We further found that Co(II) was the most preferred metal cofactor for DEC22-18.

Sequence Optimization by Nucleotide Truncation. DEC22-18 exhibited a k_{obs} of 1.0 min^{-1} under the selection buffer conditions (50 mM HEPES, pH 6.8 at 23 °C, 400 mM NaCl, 100 mM KCl, 7.5 mM $MgCl_2$, 5 mM $MnCl_2$, 1 mM $CoCl_2$, 0.25 mM $NiCl_2$, 1.25 mM $CdCl_2$). DEC22-18 is a large DNA molecule consisting of 109 nucleotides. To determine whether sequence of the DNA enzyme could be minimized, we synthesized a series of DNA molecules with variable truncations from the 3′-end. These truncated mutants were examined for catalytic activity and the results are summarized in the embedded graph in Figure 4 (relative activities are shown with that of the wild-type DEC22-18 taken as 100). We found that the last 29 nucleotides of DEC22-18 could be deleted without significantly reducing the catalytic activity. Interestingly, several truncated mutants were more effective than the wild-type molecule. For example, the truncation of the last 26 nucleotides produced an 83-nt enzyme, denoted DEC22-18A, that had significantly improved catalytic activity with a k_{obs} of 2.1 min^{-1} under the selection buffer conditions. We observed further that DEC22-18A was an even more effective catalyst when present in a solution containing 50 mM HEPES (pH 6.8 at 23 °C), 5 mM $MgCl_2$, and 10 mM $CoCl_2$, without monovalent metal ions. In this case, the self-cleavage reaction was too fast to allow an accurate measurement of the rate constant using conventional manual quenching methods. However, we estimated that the k_{obs} value was near 10 min^{-1} on the basis of the observation that nearly 50% of the DEC22-18A was cleaved in 3 s.

A *trans*-Acting DNA Enzyme. A secondary structure for DEC22-18A predicted by the M-fold program[21] is shown in Figure 5A. On the basis of this structure, we successfully designed a *trans*-acting DNA enzyme system, DET22-18, by replacing stem-1 and its loop existing in DEC22-18A with a stem made of eight base-pairs (Figure 5B). DET22-18 is a true multiple-turnover DNA enzyme that cleaves substrate S1 according to Michaelis−Menten kinetics. Figure 5C shows the data from a set of kinetic experiments where DET22-18 was used at 5 nM while the concentration of S1 was varied between 100 and 2000 nM. A k_{cat} of 7.2 ± 0.7 min^{-1} and a K_M of 0.94 ± 0.19 μM were derived using GraFit software. These data indicate that the 58-nt DET22-18 is a very efficient DNA enzyme.

Signaling Properties of DET22-18. The signaling behavior of the DET22-18/S1 system was monitored in real time via fluorescence spectroscopy. We used a less optimal Co(II) concentration (1 mM rather than 10 mM) to slow the cleavage reaction so that the fluorescence intensity changes could be monitored using the conventional spectroscopic method as well as to minimize the fluorescence quenching imposed by this metal ion (see Discussion below). The signaling reaction was examined under two different enzyme:substrate ratios: (1) DET22-18 (E) in 10-fold excess over S1 (Figure 6A) and (2) S1 in 10-fold excess over DET22-18 (Figure 6B). In both cases, the system had a constant fluorescence intensity (first 10 min of the reaction) when S1 was incubated with metal ions without DET22-18. When the DNA enzyme was introduced, the fluorescence intensity of both solutions increased sharply. In Figure 6A (E:S = 10:1), the fluorescence enhancement ($F/F0$; $F0$ was the initial intensity, and F was the intensity at any given

(21) It can be accessed at http://bioinfo.math.rpi.edu/~mfold/dna/form1.cgi.

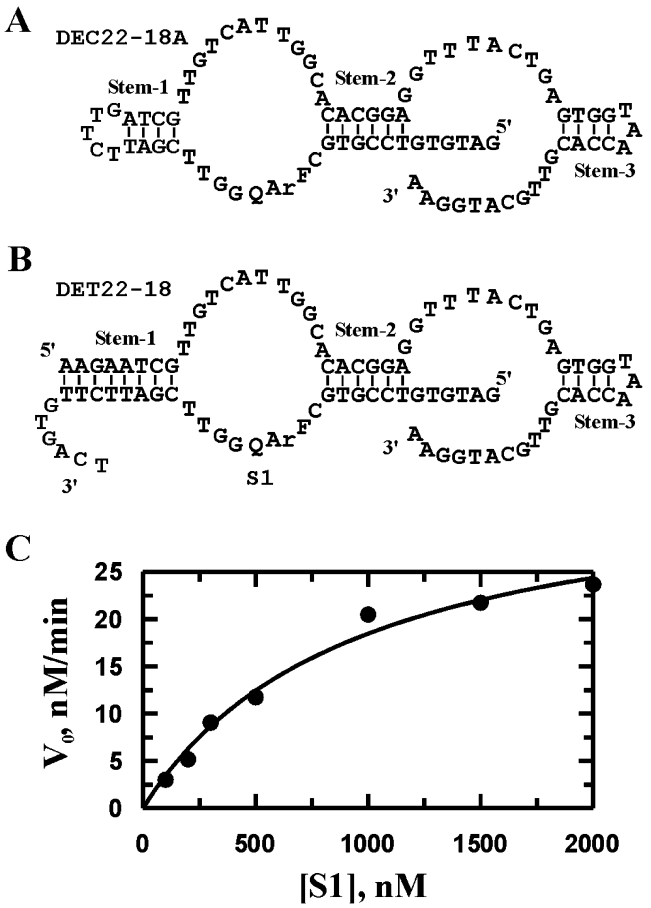

Figure 5. Structure and catalytic parameters of DET22-18. **(**A**)** A secondary structure of DEC22-18 predicted by the M-fold program. **(B)** A *trans*-acting DNA enzyme, DET22-18, which was designed on the basis of the predicted secondary structure. **(**C**)** Kinetic analysis of DET22-18. The 34-nt substrate S1 was labeled at the 5′-end with [γ-^{32}P]ATP and PNK. 5 nM of DET22-18 was incubated with S1 at 100, 200, 300, 500, 1000, 1500, and 2000 nM in the reaction buffer containing 10 mM $CoCl_2$, 5 mM $MgCl_2$, and 50 mM HEPES, pH 6.8. Aliquots were collected at different time points for determining rate constants by PAGE. The rate constants at different substrate concentrations were fit to the Michaelis−Menten equation using GraFit software. Experiments were conducted in triplicate, and the average velocity at each substrate concentration is shown in the graph.

time) increased at such a rapid rate that within 1 min, a 7.4-fold enhancement was observed (see inset graph). In Figure 6B, the fluorescence enhancement increased at a reduced rate as expected because the concentration of the DNA enzyme was 10-fold less than that of the substrate. We found 3.3-fold enhancement in 1-min incubation (see inset graph), representing an initial turnover rate of 2.1 min^{-1} (based on the observation that a 16-fold enhancement was observed when the reaction was completed). These data indicate that the signaling DNA enzyme can be used for signal generation under a broad range of substrate concentrations. It should be noted that the lower overall fluorescence enhancement relative to the cleavage experiments with NaOH shown in Figure 1B was likely due to the use of different reaction conditions as well as to the partial quenching of the fluorescence intensity by the divalent transition metal ions present in the assay buffer. Work is currently underway to characterize the effects of various metal ions on the signaling magnitude of the DET22-18/S1 system as well as to fully characterize the signaling and catalytic properties of

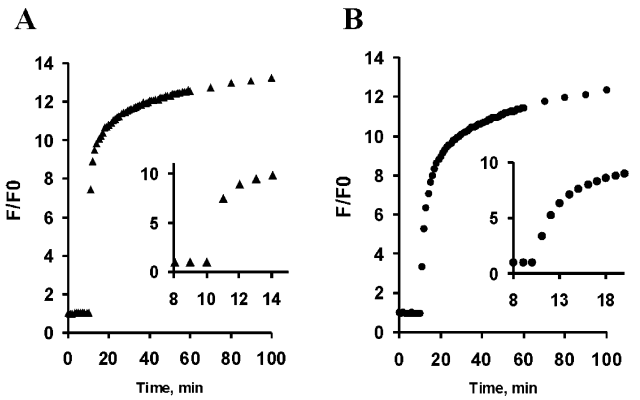

Figure 6. Examination of the real-time signaling capability of DET22-18/S1 system. (A) Deoxyribozyme DET22-18 in excess. (B) Substrate S1 in excess. S1 was incubated at room temperature in the absence of DET22-18 for 10 min, followed by the addition of DET22-18 and a further incubation at the same temperature for an additional 90 min. The fluorescence intensity was recorded every minute for the first 60 min and every 10 min thereafter. The DNA concentrations were as follows: S1 at 0.5 μM, DET22-18 at 5 μM in 5A and 0.05 μM in Figure 5B. The reaction mixture also contained 50 mM HEPES, pH 6.8 (determined at 23 °C), 14 mM $MgCl_2$, and 1 mM $CoCl_2$.

the DNA enzyme under various solution conditions, and the results will be reported elsewhere.

Design of a Signaling Allosteric DNA Enzyme. On the basis of the body of established knowledge, generated from the recent studies on the engineering of many allosteric ribozymes[22] from existing ribozymes and RNA aptamers, we hypothesized that the stem−loop feature in the structure of DEC22-18A was ideal for the design of allosteric deoxyribozymes. To test whether DEC22-18A could indeed be easily designed into an allosteric DNA enzyme, we conjugated an ATP aptamer[17] to the DNA enzyme through a weakened stem-1 (Figure 7A). In the absence of ATP, the weak stem-1 should not associate strongly, and as a result, the catalytic activity of this construct was expected to be weak. However, when ATP was introduced, the aptamer domain should form a stable complex with ATP to promote the formation of stem-1 and thereby significantly increase the cleavage activity. A similar strategy was previously used to successfully engineer an allosteric DNA enzyme.[23]

The conjugated DNA molecule was assessed for signaling properties initially under the following reaction conditions: 50 mM HEPES (pH 6.8 at 23 °C), 400 mM NaCl, 100 mM KCl, 14 mM $MgCl_2$, and 1 mM $CoCl_2$ at 23 °C (Figure 7B). The fluorescent intensity increased at a rate of ∼0.04 fluorescence units/min (f.u./min) when ATP was absent (first 5-min incubation). Upon introduction of ATP (prior to the data recording at the sixth minute of the incubation), the signaling rate increased to ∼0.16 f.u./min, a 4-fold enhancement in the catalytic rate. The system reached 80% of its maximal signaling capability in 3 min following the addition of ATP. The nature of the RNA-cleavage-dependent fluorescence signaling was confirmed by PAGE analysis of the cleavage products using a ^{32}P-labeled DNA construct, and an identical 4-fold activation of RNA cleavage induced by ATP was observed in the PAGE experiment.

The ligand-promoted rate enhancement (i.e., k_{+ATP}/k_{-ATP}) observed above was relatively small. It is apparent from the

(22) Many strategies for allosteric ribozyme engineering have been reported in the literature, which are comprehensively reviewed in ref 11.
(23) Reference 13c.

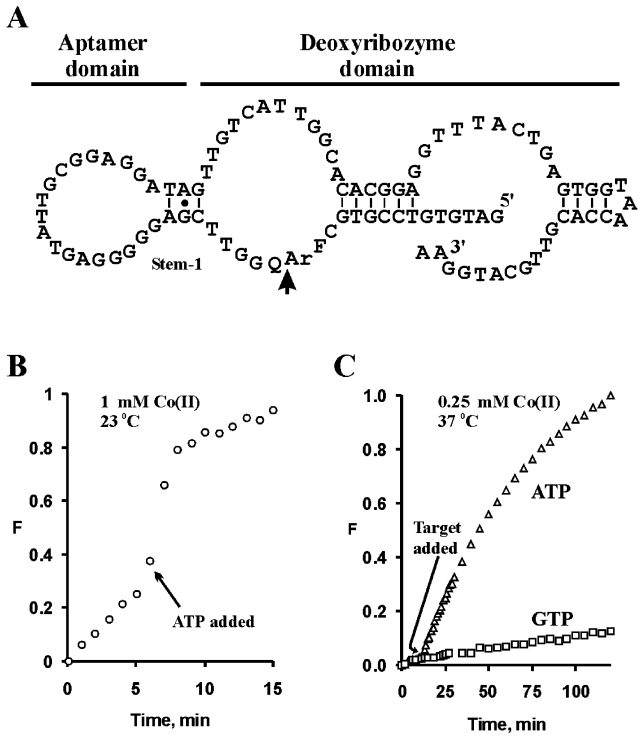

Figure 7. ATP-dependent allosteric DNA enzyme. **(**A**)** A DNA molecule conjugated using a known ATP aptamer and the signaling DNA enzyme through a weak stem-1. **(**B**)** ATP activation assay. The conjugated DNA was incubated at room temperature in the absence of ATP for 5 min, followed by the addition of ATP (to 1 mM), and a further incubation at the same temperature for 10 min. The fluorescence intensity was recorded every minute. The DNA concentration was 40 nM, and the reaction mixture contained 50 mM HEPES, pH 6.8 at 23 °C, 14 mM $MgCl_2$, and 1 mM $CoCl_2$, 400 mM NaCl, 100 mM KCl. **(**C**)** Activation by ATP and GTP. The DNA molecule was incubated at 37 °C in the absence of ATP or GTP for 10 min, followed by the addition of 1mM ATP (triangle) or GTP (square) and a further incubation at the same temperature for an additional 110 minutes. The fluorescence intensity was recorded every minute for the first 30 min and every 5 min thereafter. The reaction conditions were the same as in (B) except for $CoCl_2$, which was used at 0.25 mM. The fluorescence intensity was normalized as $(F - F_0)/(F_{max} - F_0)$ where F is the fluorescence reading of a solution at any given time point, F_0 is the reading of each sample made at the starting point, and F_{max} is the reading made either at 15 min for the sample used in (B) or at 120 min for the ATP-containing sample used in (C).

data shown in Figure 7B that the RNA cleavage activity of the aptamer−deoxyribozyme construct was high in the absence of ATP. This suggests that the enzymatic domain alone can form a sufficiently stable and active structure to facilitate efficient catalysis. We hypothesized that this ability of "self-folding" could be weakened at a higher temperature and a reduced Co^{2+} concentration. Therefore, we performed a series of experiments at elevated temperatures and decreased Co^{2+} concentrations, and the results obtained supported our hypothesis. Figure 7C illustrates the results from a set of experiments conducted at 37 °C and 0.25 mM Co^{2+} in the presence of 1 mM ATP or 1 mM GTP. Each reaction mixture was incubated in the absence of ATP or GTP for the first 10 min, and ATP or GTP was introduced before the reading was taken at the 11th minute of the reaction. In the absence of ATP, and with GTP, the reaction proceeded at the same signaling rate (initial rate) of 9.5×10^{-4} f.u./min. In the presence of ATP, the signaling rate increased to 1.8×10^{-2} f.u./min, representing a nearly 20-fold rate enhancement by ATP. The data in Figure 7C also indicated that the target reporting was ATP-specific as GTP did not produce any significant signal enhancement. We expect that signaling DNA enzymes with more responsive allosteric activation and less reduction in catalytic rate can be obtained through in vitro selection using partially randomized DEC22-18 sequences. This strategy has been successfully demonstrated in the creation of many effective allosteric ribozymes.[22] The creation of ligand-dependent, signaling DNA enzymes that show large rate enhancements in the presence of biological targets of interest will be the focus of our future efforts.

Discussion

We have created both a *cis*-acting RNA-cleaving DNA enzyme, DEC22-18, and a related *trans*-acting DNA enzyme, DET22-18, that have uniquely synchronized chemical catalysis/real-time signaling capabilities. DEC22-18 has a unique structural feature wherein the enzyme and substrate are present within the same molecule, leading to an autocatalytic system capable of generating a large fluorescence signal in the presence of appropriate divalent metal ions. An advantage of such a system is that both the catalytic and signaling components are present in a single molecule; thus, there is the potential for the development of a "reagentless" sensor by immobilization of the DNAzyme onto a suitable surface such as an optical fiber. In this case, only the presence of the appropriate target would be required to generate a signal. Given the large k_{obs} value and the potential to achieve very significant enhancement in fluorescence from this system, it is likely that rapid and sensitive detection of target molecules could be achieved with such a reporter.

The *trans*-acting DNAzyme DET22-18 is a true enzyme with a k_{cat} of ~ 7 min^{-1}, making it the second fastest DNA enzyme reported to date (the best DNA enzyme is 10-23 with a k_{cat} of ~ 10 min^{-1} under optimal conditions[7]). The 58-nt DNA enzyme cleaves a chimeric RNA/DNA substrate at the lone RNA linkage surrounded by a closely spaced fluorophore-quencher pair—a unique structure that permits the synchronization of chemical cleavage with fluorescence signaling. The short distance between F and Q gives rise to the maximal fluorescence quenching in the starting substrate (for both *cis* and *trans* reactions) and produces a very large fluorescence enhancement upon chemical catalysis. At the same time, the covalent integration of F and Q within the same substrate prohibits undesirable long-range movement of the fluorophore and the quencher away from each other so that the potential for false signaling that does not originate from chemical catalysis can be minimized. With the ability for fast chemical action, the synchronized catalysis-signaling capability, the very desirable fluorescence signaling properties (low background fluorescence, large signal enhancement, and minimal potential for false signaling), along with a simple stem−loop structure, DET22-18 is an ideal DNA enzyme for engineering useful allosteric deoxyribozyme biosensors with exceptional real-time detection sensitivity and accuracy. Moreover, it is conceivable that a large number of similar DNA enzymes carrying different fluorophores and quenchers can be created very easily with the similar strategy used for the creation of DET22-18. Such DNA enzymes will be useful in setting up various forms of multiplexed assays for the detection of important biological targets.

Acknowledgment. We thank members of Li laboratory for helpful discussions. This work was supported by research grants from Canadian Institutes of Health Research, Natural Sciences and Engineering Research Council of Canada, and Canadian Foundation for Innovation. Y.L. and J.D.B. are both holders of Canada Research Chairs.

JA0281232